Bioorganic & Medicinal Chemistry 22 (2014) 211–220

Contents lists available at ScienceDirect

Bioorganic & Medicinal Chemistry

journal homepage: www.elsevier.com/locate/bmc

Rational design and synthesis of topoisomerase I and II inhibitors based on oleanolic acid moiety for new anti-cancer drugs

Ahmed Ashour [a,b], Saleh El-Sharkawy [b,c], Mohamed Amer [b], Fatma Abdel Bar [b], Yoshinori Katakura [d], Tomofumi Miyamoto [e], Nozomi Toyota [a], Tran Hai Bang [a], Ryuichiro Kondo [a], Kuniyoshi Shimizu [a,*]

[a] Department of Agro-Environmental Sciences, Faculty of Agriculture, Kyushu University, Fukuoka, Japan
[b] Department of Pharmacognosy, Faculty of Pharmacy, Mansoura University, Mansoura, Egypt
[c] Department of Pharmacognosy, Faculty of Pharmacy, Delta University for Science and Technology, Egypt
[d] Department of Genetic Resources Technology, Faculty of Agriculture, Kyushu University, Fukuoka, Japan
[e] Graduate School of Pharmaceutical Sciences, Kyushu University, Fukuoka, Japan

ARTICLE INFO

Article history:
Received 8 October 2013
Revised 15 November 2013
Accepted 16 November 2013
Available online 25 November 2013

Keywords:
Oleanolic acid
Topoisomerase I and II
Inhibitor
SARS

ABSTRACT

Semisynthetic reactions were conducted on oleanolic acid, a common plant-derived oleanane-type triterpene. Ten rationally designed derivatives of oleanolic acid were synthesized based on docking studies and tested for their topoisomerase I and IIα inhibitory activity. Semisynthetic reactions targeted C-3, C-12, C-13, and C-17. Nine of the synthesized compounds were identified as new compounds. The structures of these compounds were confirmed by spectroscopic methods (1D, 2D NMR and MS). Five oleanolic acid analogues (**S2**, **S3**, **S5**, **S7** and **S9**) showed higher activity than camptothecin (CPT) in the topoisomerase I DNA relaxation assay. Four oleanolic acid analogues (**S2**, **S3**, **S5** and **S6**) showed higher activity than etoposide in a topoisomerase II assay. The results indicated that the C12–C13 double bond of the oleanolic acid skeleton is important for the inhibitory activity against both types of topoisomerases, while insertion of a longer chain at either position 3 or 17 increases the activity against topoisomerases by various degrees. Some of the synthesized compounds act as dual inhibitors for both topoisomerase I and IIα.

1. Introduction

Inhibition of topoisomerases is one of the most important mechanisms of anticancer drugs.[1] Pentacyclic triterpenes such as boswellic, betulinic, ursolic and oleanolic acids are reported to inhibit topoisomerases I and IIα by competing with DNA for topoisomerase binding through direct interaction with the enzyme preventing topoisomerase-DNA complex formation in both topoisomerases. The structure–activity relationship suggests that the general pentacyclic ring structure is an important system for topoisomerase inhibitory activity. Carboxylation of the pentacyclic ring structure has also been suggested to be necessary for topoisomerase inhibition.[2] Our previous work[3] resulted in isolation of oleanolic (Fig. 1) and betulinic acid as pentacylic triterpene from unused parts of *Hibiscus sabdariffa*. Based on a literature review, betulinic acid was found to be tested against topoisomerase inhibition, while the current literature included no reports of oleanolic acid derivatives as topoisomerase inhibitors. As such, oleanolic acid was suggested as a backbone for rational design of specific topoisomerase inhibitors.

Topoisomerases are universal and present in eukaryotes, archaebacteria and eubacteria.[4] They control DNA topology by cleaving and rejoining DNA strands and play an important role in regulation of the physiological function of genome.[5] Beyond their normal functions, topoisomerases are important targets, especially in the treatment of human cancer.[5] They are essential enzymes that relax DNA supercoiling inside cells during several processes like replication, recombination, and transcription. The opening of duplex DNA and separation of its two strands during transcription and replication generate supercoiling (torsional tension) on both sides of the open DNA segment. Excessive positive supercoiling tightens the DNA and prevents further strand separation, thereby stalling the polymerase. Negative supercoiling behind the polymerases, on the other hand, tends to extend DNA strand separation and facilitate the formation of abnormal nucleic acid structures. Topoisomerases prevent the formation of such potentially deleterious structures by removing free supercoiling.[1] There are two major classes of topoisomerases, type I and type II, that are distinguished by the number of DNA strands that they cleave and the mechanism by which they alter the topological properties of the genetic material.[6]

This work was conducted to facilitate the design of new analogues from oleanolic acid with enhanced activity against

* Corresponding author. Tel.: +81 92 642 3002.
E-mail address: shimizu@agr.kyushu-u.ac.jp (K. Shimizu).

0968-0896/$ - see front matter © 2013 Elsevier Ltd. All rights reserved.
http://dx.doi.org/10.1016/j.bmc.2013.11.034

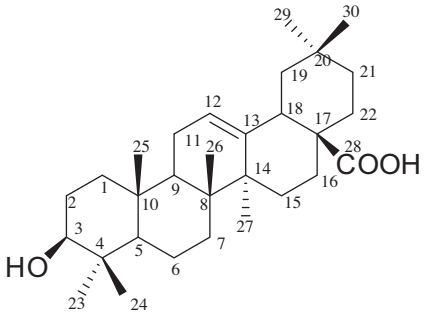

Figure 1. Structure of oleanolic acid.

topoisomerase inhibition using computer-assisted molecular modeling techniques.

2. Results and discussion

2.1. Molecular modeling and docking

To design more active analogues of oleanolic acid as topoisomerase inhibitors, a computer-aided molecular modeling study was carried out within the active site of the human topoisomerase I and IIα, starting with the crystal structure of the enzyme bound to DNA (PDB 1t8i and 1bgw for topoisomerase I and IIα, respectively).[7,8] The active site of topoisomerase enzymes is an arginine- and lysine-rich pocket with condensed positive charge that allows electrostatic interactions with the negatively charged DNA-phosphate backbone.[9] The C-28 COOH group of oleanolic acid represents the exclusive binding pharmacophore, generating a hydrogen-bonding interaction with the structural skeleton, but it is too short to bridge to the other side of the enzyme (Fig. 2A), so our study depends mostly on elongation of the chain at the substituents at positions 3 and 17 (Fig. 2B). Based on this idea, several analogues of oleanolic acid were proposed (Fig. 3). The tautomeric forms of these designed structures were calculated using Marvin Suite (ChemAxon, Budapest, Hungary) at assay pH and then docked to topoisomerase I and IIα active sites. The structures of the topoisomerase I and II inhibitors camptothecin (CPT) and etoposide, respectively, were used as reference molecules in docking and modeling studies (Fig. 4).

The proposed molecules were docked to topoisomerase I and II active sites. The results are shown in Table 1. From these results, it was found that the proposed structures have a good ability to inhibit both topoisomerase I and II. It was also found that some structures have high binding affinity to both types of enzymes, which means that these compounds can act as dual inhibitors for topoisomerase I and II. This ability is very useful for cancer inhibition, as specific topoisomerase I and II inhibitors are able to cause permanent DNA damage.

Given that both enzymes are good targets, it would be desirable to jointly inhibit them, but use-limiting toxicity of sequential or simultaneous combinations of topoisomerase I and II poisons include severe to life-threatening neutropenia and anemia. Furthermore, the emergence of resistance phenomena to topoisomerase I inhibitors is often accompanied by a concomitant rise in the level of topoisomerase II expression and vice versa, leading to the failure of clinical therapies.[10] In this regard, a single compound able to inhibit both topoisomerase I and II may present the advantage of improving antitopoisomerase activity, with reduced toxic side effects, with respect to the combination of the two inhibitors. These compounds will therefore be synthesized and their activities against topoisomerase I and II will be confirmed using an in vitro assay.

2.2. Semisynthesis of oleanolic analogues (S1–S10)

Compounds **S1**–**S10** were prepared (Schemes 1 and 2) after having a preliminary idea about their activity using the molecular modeling as mentioned before.

Reaction of *m*-chloroperoxybenzoic acid with oleanolic acid afforded product **S1**. ^{1}H and ^{13}C NMR data of **S1** suggested the disappearance of the double bond of oleanolic acid. ^{13}C NMR is the same as oleanolic acid except that two signals of double bond are replaced by two signals at δ_c 90.6 and 76.4. ^{1}H NMR spectrum of **S1** showed one oxygenated proton at δ_H 3.89 (H-12) which is differ from oleanolic acid. This proton correlated with carbon signal at δ_c 76.4 (C-12) in HMQC spectrum and showed HMBC correlations with the carbon signals at δ_c 42.3 (C-14), 44.6 (C-9), 51.1 (C-18), 90.5 (C-13). These correlations confirmed the position of this proton. The FAB–MS of this compound (positive-ion mode) displayed peak at m/z = 473 $[M+H]^+$ while negative-ion mode displayed peak at m/z at 471 $[M-H]^+$ suggesting a molecular formula $C_{30}H_{48}O_4$. Comparing the previous data (^{13}C, ^{1}H NMR, $[\alpha]_D^{24}$ and mass) with similar published data,[11] compound **S1** was determined to be oleanderolide.

Carbamoylation of oleanolic acid by reaction with different isocyanates afforded compounds **S2**–**S9**. Down field shift of the H-3 and C-3 signals in **S2** (+1.30 and +5.6 ppm, respectively) compared to that of the starting material (oleanolic acid) suggested a possible carbomylation at C-3. The NMR data (Table 2) further supported this fact and were closely comparable to those of oleanolic acid with additional C-3-*O*-[*N*-(benzyl) carbomyl] moiety signals.

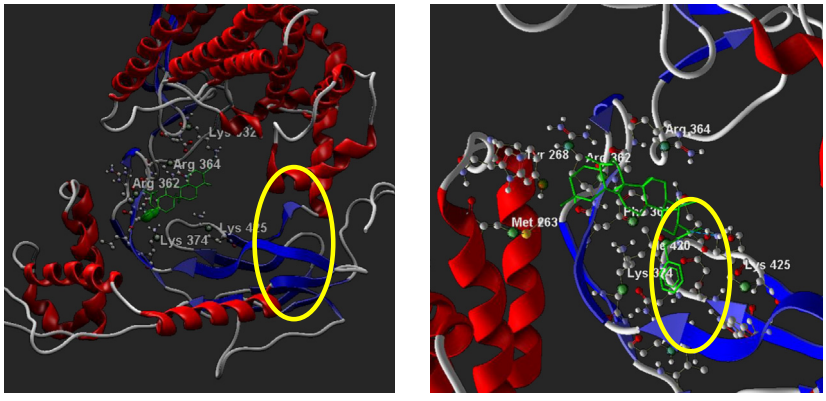

(A) **(B)**

Figure 2. Detailed view of docked structure oleanolic acid (A) and **S2** (B) as one example of the proposed structures with the corresponding interacting amino acids of topoisomerase I binding sites.

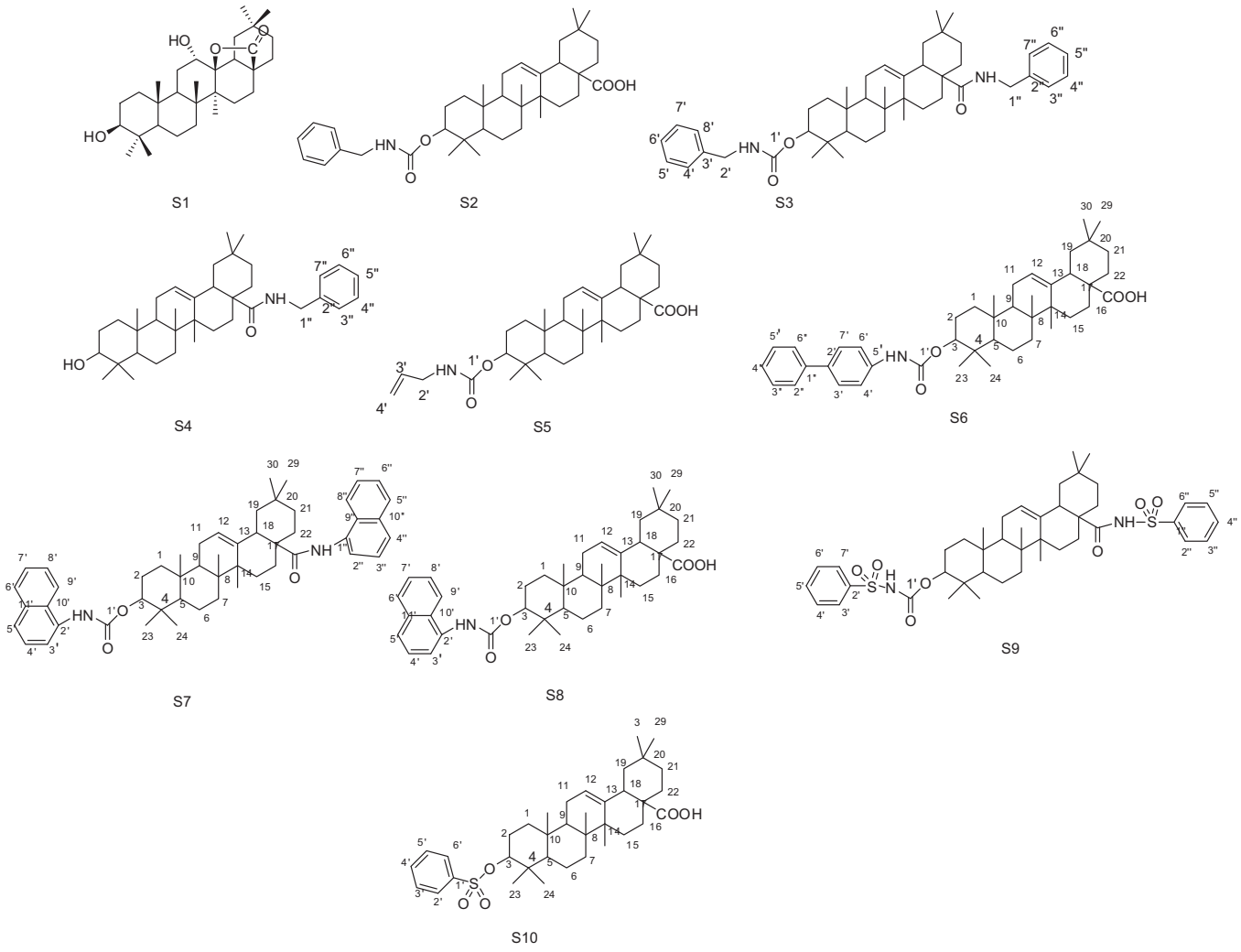

Figure 3. Oleanolic acid analogues designed for molecular modeling.

Protons and carbons assignments were further confirmed using HMQC spectrum. The carbonyl carbon at δ_c 157.1 was assigned to C-1′ on the basis of its ^2J-HMBC correlation with the broad singlet H-2′ (δ_H 4.50). Proton H-2′ also showed ^2J-HMBC with the quaternary C-3′ (δ_c 138.4) and ^3J-HMBC correlation with the methine carbon C-4′ and C-8′ (δ_c 127.4). The proton signal H-4′/8′ (δ_H 7.26) showed HMBC correlation with the methine carbon C-6′ (δ_c 127.5) while H-5′/7′ signal (δ_H 7.32) showed a correlation with the quaternary carbon C-3′ (δ_c 138.4). The FAB–MS of this compound (negative-ion mode) displayed peak at m/z at 588 $[M-H]^+$ suggesting a molecular formula $C_{38}H_{55}NO_4$. Thus compound **S2** was proved to be 3-*O*-[*N*-(benzyl) carbamoyl]-oleanolic acid.

Down field shift of the H-3 and C-3 signals in **S3** (+1.30 and +5.6 ppm, respectively) compared to that of the starting material (oleanolic acid) suggested a possible carbomylation at C-3. The ^{13}C NMR data (Table 2) showed an upfield shift of the quaternary carbon C-28 (−7.9 ppm) compared to that of oleanolic acid, suggesting a possible reaction at this position. The NMR data further supported this fact and were closely comparable to those of oleanolic acid with additional C-3-*O*-[*N*-(benzyl)carbomyl] moiety and 17β-*O*-[*N*-(benzyl)carbomyl] moiety signals. Protons and carbons assignments were further confirmed using HMQC spectrum. The carbonyl carbon at δ_c 154.8 was assigned to C-1′ on the basis of its ^2J-HMBC correlation with the broad singlet H-2′ (δ_H 4.52). Proton H-2′ also showed ^2J-HMBC with the quaternary C-3′ (δ_c 138.4) and ^3J-HMBC correlation with the methine carbon C-4′ and C-8′ (δ_c 128.3). The proton doublet H-4′/8′ (δ_H 7.34) showed HMBC correlation with the methine carbon C-6′ (δ_c 126.9) while H-5′/7′ (δ_H 7.22) signal showed a correlation with the quaternary carbon C-3′ (δ_c 138.4). The carbonyl carbon at δ_c 172.9 was assigned to C-28 on the basis of its ^2J-HMBC correlation with the broad singlet H-1″ (δ_H 4.98). Proton H-1″ also showed ^2J-HMBC with the quaternary C-2″ (δ_c 138.7) and ^3J-HMBC correlation with the methine carbon C-3″ and C-7″ (δ_c 128.6). The proton signal H-3″/7″ (δ_H 7.33) showed HMBC correlation with the methine carbon C-5″ (δ_c 127.4). EI-MS spectrum showed molecular ion peak at m/z 678 $[M]^+$. This suggests the empirical formula to be $C_{45}H_{62}N_2O_3$. Thus compound **S3** was proved to be 3-*O*-[*N*-(benzyl)carbamoyl]-17β-*O*-[*N*-(benzyl)carbomyl]-oleanolic acid.

Chemical shift of the H-3 and C-3 signals in **S4** is nearly the same compared to that of the starting material (oleanolic acid) suggested no carbomylation reaction occur at C-3 while the ^{13}C NMR data (Table 2) showed an upfield shift of the quaternary carbon C-28 (−7.9 ppm) compared to that of oleanolic acid, suggesting a possible reaction at this position. The NMR data further supported this fact and were closely comparable to those of oleanolic acid with additional 17β-*O*-[*N*-(benzyl)carbomyl] moiety signals. Protons and carbons assignments were further confirmed using HMQC spectrum. The carbonyl carbon at δ_c 172.9 was assigned to C-28 on the basis of its ^2J-HMBC correlation with the

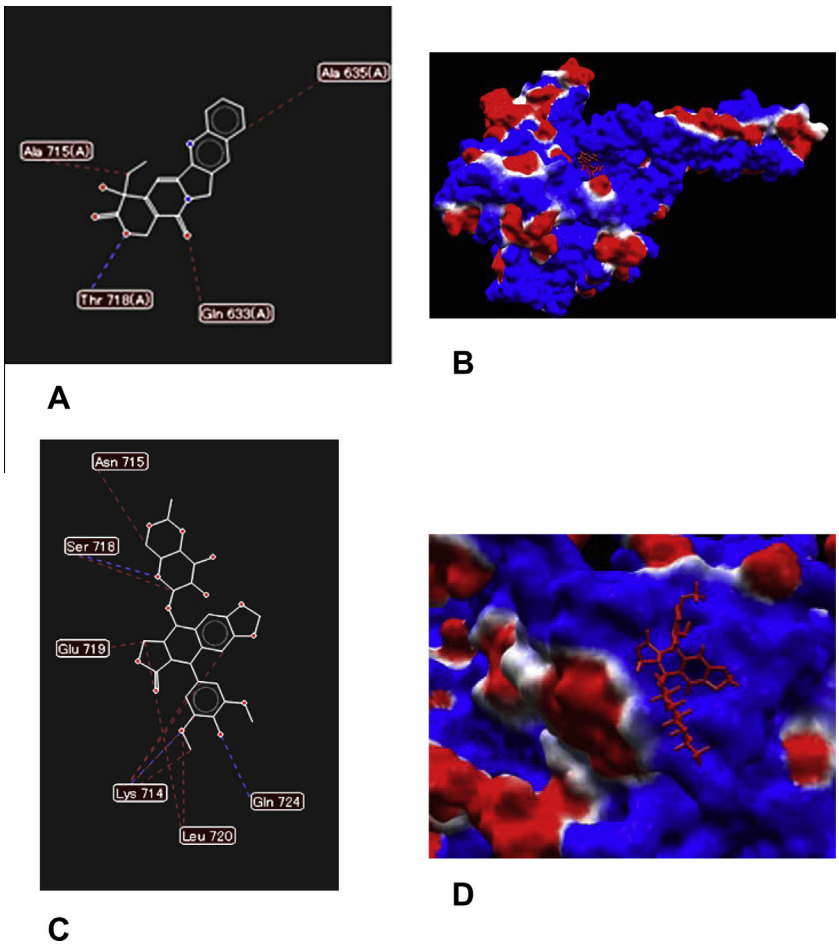

Figure 4. Detailed view of docked structures of camptothecin and etoposide with topoisomerase I and II respectively (A) binding sites of CPT, (B) complex structure of CPT with topoisomerase I, (C) binding sites of etoposide, (D) complex structure of etoposide with topoisomerase II.

Table 1
Comparison of energy scores for different compounds with topoisomerase I and II

	Topoisomerase I			Topoisomerase II		
	E_{inter}	E_{intra}	E_{score}	E_{inter}	E_{intra}	E_{score}
Camptothecin	−114.9	15.2	−99.7	—	—	—
Etoposide	—	—	—	−163.8	5.5	−158.3
Oleanolic acid	−87.6	−8.5	−96.1	−116.9	−8.9	−125.9
S1	−95.09	5.1	−89.8	−124.6	5.2	−119.4
S2	−124.9	−5.3	−130.3	−156.7	17.0	−173.7
S3	−139.1	−8.8	−147.9	−161.1	−1.8	−162.9
S4	−115.9	−7.3	−123.3	−131.9	−4.3	−136.2
S5	−129.6	1.7	−127.8	−133.8	5.31	−128.5
S6	−146.0	2.7	−143.3	−173.4	−2.71	−176.1
S7	−163.9	0.8	−163.1	−184.1	2.9	−181.2
S8	−164.2	7.2	−157.0	−205.9	−−0.5	−206.4
S9	−103.5	−30.7	−134.2	−168.2	−23.3	−191.5
S10	−120.5	−2.7	−123.2	−147.7	−8.7	−156.4

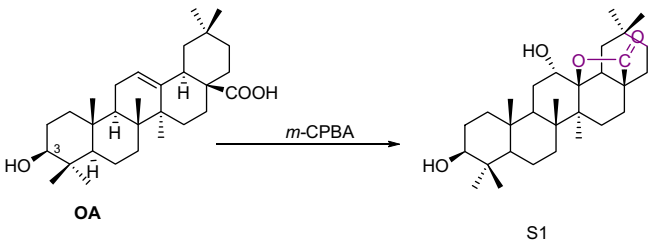

Scheme 1. Preparation of compound **S1**.

broad singlet H-1″ (δ_H 4.42). Proton H-1″ also showed ^2J-HMBC with the quaternary C-2″ (δ_c 138.7) and ^3J-HMBC correlation with the methine carbon C-3″ and C-7″ (δ_c 127.5). The proton signal H-3″/7″ showed HMBC correlation with the methine carbon C-5″ (δ_c 127.4). The proton signal H-4″/6″ showed HMBC correlation with the methine carbon C-2″ (δ_c 138.7). EI-MS spectrum showed molecular ion peak at m/z 545 $[M]^+$. This suggests the empirical formula to be $C_{37}H_{55}NO_2$. Thus compound **S4** was proved to be 17β-*O*-[*N*-(benzyl)carbomyl]-oleanolic acid.

The ^1H and ^{13}C NMR data (Table 2) of **S5** suggested close similarity to oleanolic acid with an additional C-3-*O*-[(*N*-allyl)carbomyl] moiety. This suggestion was further confirmed by HMQC and HMBC spectrum. The nitrogenated methylene carbon C-2′ (δ_c 43.4) was assigned based on HMBC correlation with H-4′a and H-4′b. The olefinic methine carbon C-3′ (δ_c 134.8) showed HMBC correlation with H-4′ and H-2′. Also the olefinic methylene carbon showed HMBC correlation with H-2′. All of these assignments confirmed the allyl side chain. The FAB–MS of this compound (negative-ion mode) displayed peak at m/z at 538 $[M-H]^+$ suggesting a molecular formula $C_{34}H_{53}NO_4$. Thus compound **S5** was proved to be 3-*O*-[*N*-(allyl)carbamoyl]-oleanolic acid.

Down field shift of the H-3 of **S6** compared to that of oleanolic acid confirming biphenyl carbamoylation at C-3. Due to the steric effect of the bulky biphenyl carbamoyl group[12], the ^{13}C NMR spectrum revealed line broadening of three carbon signals for C-3, C-1′, and C-3′,7′. Assignment of these carbons was based on extensive analysis of HMBC and HMQC data. The biphenyl system was further confirmed via HMBC correlation of the proton H-3′, 7′ (δ_H

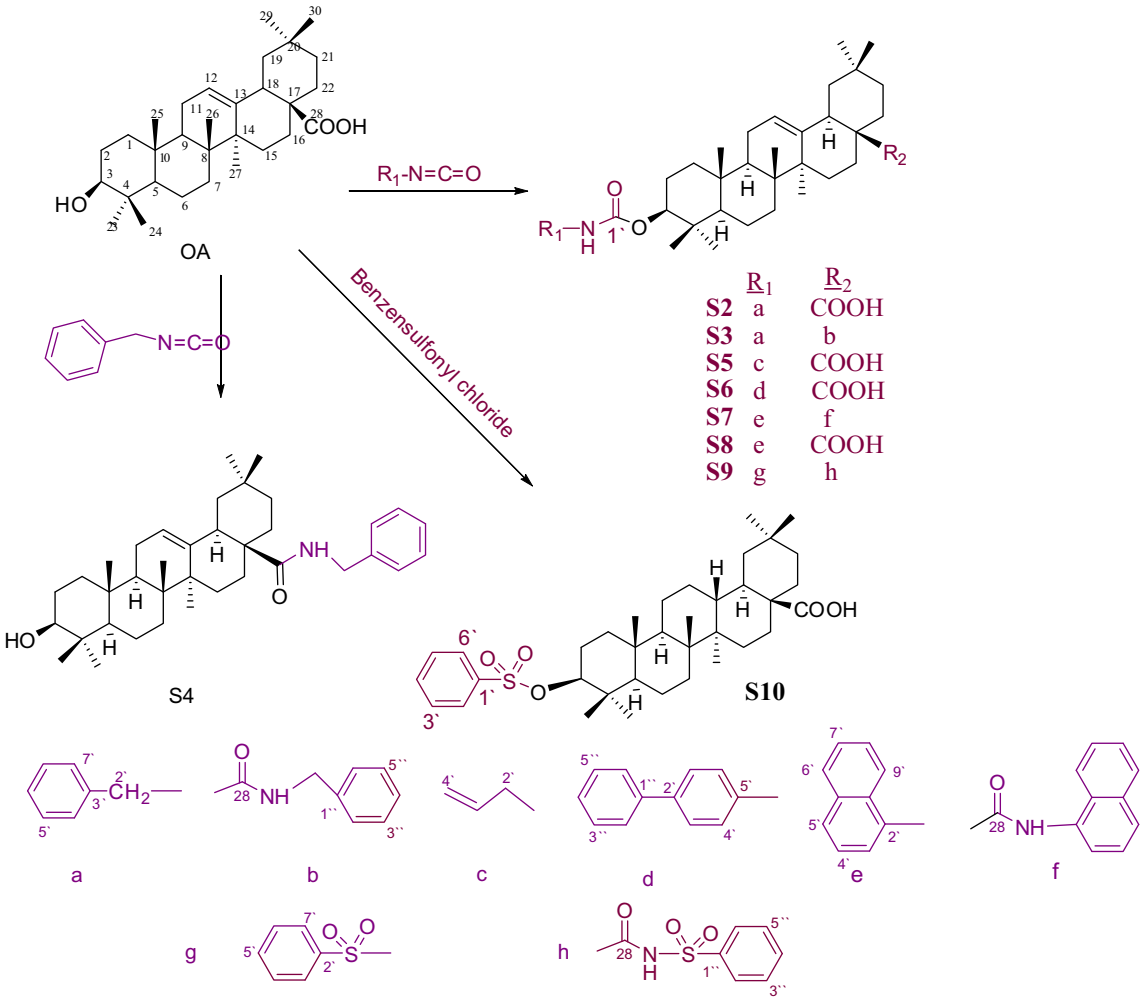

Scheme 2. Preparation of compound **S2–S10**.

7.46) with the quaternary carbon signal at δ_c 140.6 (C-1″) and the proton H-2″,6″ (δ 7.57) with the quaternary carbon C-2′ (δ_c 137.4). The FAB-MS of this compound (negative-ion mode) displayed peak at m/z at 650 $[M-H]^+$ suggesting a molecular formula $C_{43}H_{57}NO_4$. Thus, the structure of **S6** was determined to be 3-*O*-[*N*-(biphenyl)-*p*-carbamoyl]-oleanolic acid.

The ^{1}H NMR of **S7** spectrum showed a downfield shift of H-3 (+1.44) compared to oleanolic acid, suggesting carbamoylation at C-3. The ^{13}C NMR data (Table 2) showed an upfield shift of the quaternary carbon C-28 (−6.9) compared to that of oleanolic acid, suggesting a possible reaction at this position. Careful assignment of ^{13}C NMR spectrum revealed line broadening of several carbon signals. These carbon signals were identified through both HMQC and HMBC spectra. In HMQC spectrum, the carbamoylation position (C-3), showed a cross peak of H-3 (δ_H 4.56) and a broad carbon signal at δ_c 83.0. Similarly, the proton signals at δ_H 7.88 showed cross peaks in HMQC with broad carbon signals at δ_c 120.8 (C-6′). Proton H-4′ and H-5′ confirmed this assignment through their HMBC correlations with C-5′ and C-6′, respectively. HMBC spectrum revealed third and fourth very broad quaternary carbon signal at δ_c 134.0 (C-2′), which was correlated with both H-4′ and H-9′ and broad carbon signal at δ_c 132.8 (C-1″), which was correlated with both H-8″ and H-3″. The carbonyl carbon C-1′ was assigned to be the fifth broad signal at δ_c 157.0. The line broadening of these carbons may be attributed to the steric effect of the bulky naphthyl carbamoyl moiety.[12] The FAB–MS of this compound (positive-ion mode) displayed peak at m/z = 751 $[M+H]^+$ while negative-ion mode displayed peak at m/z at 749 $[M-H]^+$ suggesting a molecular formula $C_{51}H_{62}N_2O_3$. Thus, the structure of S7 was proved to be 3-*O*-[*N*-(1-naphthyl)-carbamoyl]-17-β-[*N*-(1-naphthyl)-carbamoyl]-oleanolic acid.

The ^{1}H NMR spectrum of **S8** showed a downfield shift of H-3 (+1.44) suggesting a possible carbamoylation at C-3. Careful assignment of ^{13}C NMR spectrum revealed line broadening of five carbon signals. These carbon signals were identified through both HMQC and HMBC spectra. In HMQC spectrum, the carbamoylation position (C-3), showed a cross peak of H-3 (δ_H 4.56) with a broad carbon signal at δ_c 83.5. Similarly, the proton signals at δ_H 7.64 and 7.90 showed cross peaks in HMQC with broad carbon signals at δ_c 124.0 and 121.0 (C-5′ and C-6′). COSY spectrum was used for confirmation of the assignment of the aromatic protons. Proton H-4′ and H-5′ confirmed this assignment through their HMBC correlations with C-5′ and C-6′, respectively. HMBC spectrum revealed a fourth very broad quaternary carbon signal at δ_c 134.2 (C-2′), which was correlated with both H-4′ and H-9′. The carbonyl carbon C-1′ was assigned to be the fifth broad signal at δ_c 156.7. The line broadening of these carbons may be attributed to the steric effect of the bulky naphthyl carbamoyl moiety.[12] The FAB–MS of this compound (positive-ion mode) displayed peak at m/z = 626 $[M+H]^+$ while negative-ion mode displayed peak at m/z at 624

Table 2
^{13}C NMR (150 MHz) data of compounds **S2**–**S10**

C	S2	S3	S4	S5	S6	S7	S8	S9	S10
1	37.7	38.0	37.9	37.9	37.9	37.9	38.0	37.8	38.2
2	27.4	27.4	27.5	27.7	27.7	27.4	27.7	27.6	27.6
3	84.6	84.6	81.5	81.4	83.4	83.0	83.5	85.1	91.2
4	38.0	38.2	38.2	38.0	38.1	38.2	38.1	37.8	38.5
5	55.2	55.3	55.4	55.3	55.4	55.3	55.4	55.2	55.5
6	18.1	18.1	18.2	18.2	18.2	18.1	18.2	18.1	18.3
7	32.6	32.6	33.0	33.1	33.1	32.9	32.5	32.4	32.5
8	39.4	39.4	39.4	39.3	39.3	39.5	39.3	39.2	39.2
9	47.5	47.4	47.5	47.5	47.6	47.9	47.5	47.4	47.5
10	36.8	36.8	36.9	36.9	37.0	36.8	37.0	36.9	36.8
11	23.4	23.4	23.5	23.4	23.4	23.6	23.4	22.8	23.3
12	122.8	122.8	123.0	122.5	122.6	123.1	122.5	122.4	122.4
13	143.2	143.2	143.2	143.6	143.6	144.9	143.6	143.6	143.6
14	41.7	41.7	41.8	41.5	41.6	43.0	41.6	41.5	41.6
15	27.8	27.8	28.0	28.0	23.9	23.8	23.9	23.6	24.8
16	23.6	23.6	23.6	23.6	22.9	23.5	22.9	22.6	22.9
17	46.7	47.5	47.5	46.5	46.5	47.5	46.5	46.5	46.5
18	41.2	41.2	41.3	40.9	41.0	42.3	41.0	40.9	41.0
19	45.7	45.7	45.7	45.8	45.8	46.9	45.9	45.8	45.8
20	30.6	30.7	30.7	30.7	30.7	30.7	30.6	30.6	30.6
21	33.6	33.6	33.6	33.8	33.8	34.2	33.8	33.7	33.8
22	33.0	33.0	32.6	32.4	32.4	32.4	32.4	31.6	32.4
23	27.8	28.0	28.0	28.0	28.1	28.1	28.1	27.9	27.9
24	16.8	16.8	16.7	17.1	17.1	17.0	16.7	16.6	17.1
25	17.1	17.2	17.1	16.7	16.8	16.7	17.1	17.1	16.3
26	15.2	15.3	15.3	15.4	15.4	15.4	15.4	15.4	15.3
27	25.8	25.8	25.8	25.9	25.9	25.9	25.9	25.9	25.9
28	179.9	172.9	172.9	184.1	183.4	176.6	183.6	171.4	182.9
29	31.4	31.4	31.4	32.5	32.5	33.0	33.0	33.0	33.0
30	22.9	23.0	23.9	23.9	23.6	23.7	23.6	23.3	23.5
1z	157.1	154.8		156.6	154.8	157.0	156.7	150.7	137.9
2′	44.8	45.0		43.4	137.4	134.0	134.2	137.2	127.6
3′	138.4	138.4		134.8	119.5	125.7	125.7	127.9	129.0
4′	127.4	128.3		115.9	127.7	125.7	125.7	129.3	133.3
5′	128.6	126.7			136.1	124.8	124.0	140.6	129.0
6′	127.5	126.9			127.7	120.8	121.0	129.3	127.6
7′	128.6	126.7			119.5	126.0	126.1	127.9	
8′	127.4	128.3				126.1	125.9		
9′						128.9	128.7		
10′						132.7	132.7		
11′						134.1	134.1		
1		46.7	45.1		140.6	132.8		139.2	
2″		138.7	138.7		126.8	125.9		129.4	
3″		128.6	127.5		128.8	125.9		129.3	
4″		127.5	128.6		127.0	119.9		140.5	
5″		127.4	127.4		128.8	119.3		129.3	
6″		127.5	128.6		126.8	126.0		129.4	
7”		128.6	127.5			126.0			
8″						128.7			
9″						124.8			
10″						126.5			

$[M-H]^+$ suggesting a molecular formula $C_{41}H_{55}NO_4$. Thus, the structure of **S8** was proved to be 3-*O*-[*N*-(1-naphthyl)-carbamoyl]-oleanolic acid.

The down field shift of H-3 and C-3 signals in **S9** versus those of oleanolic acid suggested a possible carbamoylation at C-3. The ^{13}C NMR data (Table 2) showed an upfield shift of the quaternary carbon C-28 compared to that of oleanolic acid, suggesting a possible reaction at this position. The reaction of organic acids' COOH groups with sulfonyl isocyanates to produce *N*-acylsulfonylamides was previously documented.[13] The assignment of the protons and carbons of the two aromatic moieties were determined based on HMQC and HMBC data. Proton H-4′,6′ (δ_H 7.47) showed a correlation with the quaternary carbon at δ_c 137.2 (C-2′), while protons H-3′, 7′ (δ_H 7.87) showed correlation with the aromatic carbon at δ_c 140.6 (C-5′). Proton H-3″, 5″ (δ_H 7.49) showed a correlation with the aromatic carbon at δ_c 139.2 (C-1″), while protons H-2″, 6″ (δ_H 7.96) showed a correlation with the aromatic carbon at δ_c 140.5 (C-4″). EI-MS spectrum showed molecular ion peak at *m*/*z* 778 $[M]^+$. This suggests the empirical formula to be $C_{43}H_{58}N_2O_7S_2$. Thus compound **S9** was proved to be 3-*O*-[*N*-(phenylsulfonyl)-carbamoyl-17β-*N*-(phenylsulfonyl)amide]-oleanolic acid.

Reaction of benzene sulfonyl chloride with oleanolic acid afforded compound **S10**. The ^{1}H NMR showed five aromatic protons H-2′,6′ (δ_H 7.91), H-3′,5′ (δ_H 7.51), and H-4′ (δ_H 7.61). The ^{13}C NMR data (Table 2) showed three methine carbons at δ_c 127.6 (C-2′,6′), δ_c 129.0 (C-3′,5′) and 133.3 (C-4′) in addition to quaternary one at δ_c 137.9 (C-1′), confirming the benzene sulfonyl moiety. HMBC correlations of the methyl singlets (H-23 and H-24) with the downfield oxymethine carbon signals at δ_c 91.2 (C-3), confirming benzenesulfonation at C-3. Further confirmation of assignment of protons and carbons was obtained using HMQC and HMBC spectrum. COSY spectrum was used for confirmation of the assignment of the aromatic protons. The FAB–MS of this compound (negative-ion mode) displayed peak at *m*/*z* at 595 $[M-H]^+$ suggesting a molecular formula $C_{36}H_{52}O_5S$. Thus compound **S10** was proved to be 3-*O*-(benzenesulfonyloxy)-oleanolic acid.

2.3. Topoisomerase I-DNA relaxation assay[14]

Inhibition of the topoisomerase function constitutes a useful strategy for the identification of potential antitumor agents. Oleanolic acid derivatives were tested using a topoisomerase I-DNA relaxation assay and compared to the known natural topoisomerase I inhibitor CPT. Reaction mixtures were analyzed by agarose gel electrophoresis. Figure 5A and Table 3 show the catalytic inhibition of topoisomerase I by oleanolic acid and its derivatives (**S1**–**S10**), as shown in lane 5–14 at 100 μM in comparison to 100 μM camptothecin (lane 4). Compound **S4** (Fig. 4A, lane 8) showed topoisomerase I inhibitory activity comparable to CPT with IC_{CPT100} 100 μM (the concentration of the compound exhibiting activity similar to that of 100 μM CPT is defined as IC_{CPT100}). Compounds **S2**, **S3**, **S5**, **S7** and **S9** (Fig. 4A, lane 6, 7, 9, 11 and 13) showed topoisomerase I inhibitory activities toward relaxation of supercoiled DNA with activity higher than that of CPT itself with IC_{CPT100} values of 16.13, 25.4, 15.23, 17.4 and 23.1 μM, respectively, compared to oleanolic acid (IC_{CPT100} 265 μM). We used IC_{CPT100} in order to find a

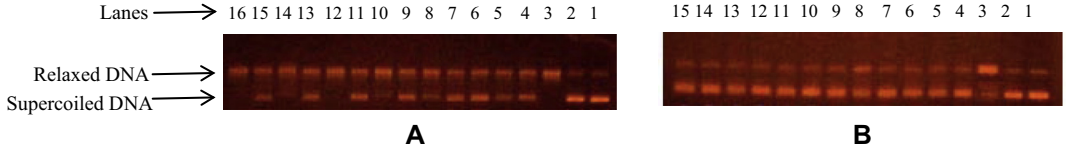

Figure 5. (A) Catalytic inhibition of topoisomerase I by oleanolic acid derivatives. Lane 1, supercoiled DNA alone (250 ng); lane 2, same as lane 1 + 0.5% DMSO; lane 3, same as lane 1 + topoisomerase I (2 U); lane 4, topoisomerase I (2 U) + 100 μM camptothecin and DNA. Lane 5–14, topoisomerase I (2 U) + DNA and 100 μM oleanolic acid analogues: lane 5 (**S1**); lane 6 (**S2**); lane 7 (**S3**); lane 8 (**S4**); lane 9 (**S5**); lane 10 (**S6**); lane 11 (**S7**); lane 12 (**S8**); lane 13 (**S9**); lane 14 (**S10**); lane 15 (oleanolic acid); lane 16 (relaxed DNA). (B) Catalytic inhibition of topoisomerase II by oleanolic acid derivatives. Lane 1, supercoiled DNA alone (250 ng); lane 2, same as lane 1 + 0.5% DMSO; lane 3, same as lane 1 + topoisomerase II (2 U); lane 4, topoisomerase I (2 U) + 100 μM etoposide and DNA. Lane 5-14, topoisomerase I (2 U) + DNA and 100 μM oleanolic acid analogues: lane 5 (**S1**); lane 6 (**S2**); lane 7 (**S3**); lane 8 (**S4**); lane 9 (**S5**); lane 10 (**S6**); lane 11 (**S7**); lane 12 (**S8**); lane 13 (**S9**); lane 14 (**S10**); lane 15 (oleanolic acid).

Table 3
Topoisomerase I and II inhibitory activity of oleanolic acid and its analogues (**S1**–**S10**)

Compound	Topoisomerase I inhibition[a] (100 μM)	Topoisomerase I inhibition relative to CPT[b]	Topoisomerase II inhibition[a] (100 μM)	Topoisomerase II inhibition relative to etoposide[b]
Oleanolic acid	6.5	0.84	5.9	0.74
S1	6.0	0.77	7.7	0.97
S2	12.7	1.64	8.9	1.12
S3	11.0	1.42	9.6	1.21
S4	7.6	0.98	8.5	1.07
S5	12.1	1.57	10.0	1.26
S6	6.1	0.79	9.6	1.21
S7	12.0	1.55	8.5	1.07
S8	3.1	0.40	8.2	1.03
S9	10.5	1.36	7.2	0.91
S10	4.2	0.54	7.3	0.92
CPT	7.7	1	ND	ND
Etoposide	ND	ND	7.9	1

[a] Topoisomerase inhibitory activity was analyzed by measuring the intensity of supercoiled DNA using imageJ software, with the positive control drug CPT (topoisomerase I assay) or etoposide (topoisomerase II assay).
[b] Values were standardized by dividing the value of intensity of each compound by the value of CPT or etoposide in topoisomerase I and II, respectively.

method to standardize the activity of these compounds due to the difficulty of determining the IC_{50} value.

2.4. Topoisomerase II-DNA relaxation assay[14]

Oleanolic acid derivatives were tested using a topoisomerase II DNA relaxation assay alongside etoposide as a positive control. Reaction mixtures were analyzed by agarose gel electrophoresis. Figure 5B and Table 3 show the catalytic inhibition of topoisomerase II by oleanolic acid derivatives (**S1**–**S10**), as shown in lanes 5–14 at 100 μM in comparison to 100 μM etoposide (lane 4).

Compounds **S1**, **S4**, **S7**, and **S8** (Fig. 5B, lane 5, 8, 11 and 12) showed topoisomerase II inhibitory activity comparable to that of etoposide with $IC_{etoposide}$ 100 μM (the concentration of the compound exhibiting activity similar to that of 100 μM etoposide is defined as $IC_{etoposide}$). Compounds **S2**, **S3**, **S5** and **S6** (Fig. 5B, lane 6, 7, 9 and 10) showed topoisomerase II inhibitory activities toward relaxation of supercoiled DNA higher than that of etoposide itself with $IC_{etopside}$ of 68.03, 56.99, 52.98 and 46.52 μM, respectively, compared to oleanolic acid ($IC_{etoposide}$ 275.8 μM).

From these results, we have concluded that the double bond between C-12 and 13 is important for anticancer activity, as compound **S1** has lower activity against topoisomerase I and slightly higher activity against topoisomerase II. In contrast, insertion of a nonpolar moiety at C-3 or C-17 significantly increased the activity against both topoisomerase I and II, with the exception of compounds **S8** and **S10**, which showed lower activity against topoisomerase I despite insertion of a longer chain. We do not have a full explanation for the behavior of these two compounds, as our study did not include consideration of the kinetic mechanism and focused only on the development of active inhibitory compounds against topoisomerase enzymes. The mechanism by which these compounds inhibits topoisomerase may be examined in our future study.

3. Materials and methods

3.1. General experimental procedure

Optical rotations were determined on JASCO, DIP-730 digital polarimeter. The ^{1}H, ^{13}C, HMBC and HMQC NMR spectra were analyzed on JEOL JNM ECA at 600 MHz for ^{1}H and 150 MHz for ^{13}C NMR spectra. FAB–MS and EI-MS were conducted at Kasuga-shi, Kyushu University. TLC was performed on aluminum sheets precoated with 0.2-mm silica gel 60 F254 (Merck). Plates were developed in a solvent mixture of *n*-hexane-ethyl acetate (9:1 and 8:2, v/v), and the developed chromatograms were visualized under 254-nm UV light and the spots were made visible by spraying with vanillin/H_2SO_4 reagent before warming in an oven preheated to 110 °C for 5 min. Silica gel 60 (Wako), 75–150 mesh, was used for column chromatography.

3.2. Plant material

Oleanolic acid was isolated and purified from a methanolic extract of unused parts of *Hibiscus sabdariffa* grown in Egypt.[3]

3.3. Preparation of compound S1[15]

To a solution of oleanolic acid (90 mg, 0.2 mmol) in methylene chloride (2.5 mL) was added 70% *m*-chloroperoxybenzoic acid (*m*-CPBA) (59 mg, 0.24 mmol). The solution was stirred for 1 h at room temperature and monitored by TLC [silica gel, petroleum ether–EtOAc (90:10)]. The reaction was stopped by addition of 10% aqueous sodium sulfite (10 mL). The aqueous solution was extracted twice with methylene chloride. The combined organic layers were washed with saturated sodium bicarbonate, and then dried under vacuum. The product was further purified by chromatography on silica gel column previously packed in petroleum ether and isocratically eluted with 10% ethyl acetate in petroleum ether. The effluents, 10 mL fractions, were monitored by TLC on silica gel plates, and similar fractions were pooled. Sub-fractions 22–24 afforded compound **S1** (13 mg, 13%) and its purity was confirmed by TLC plate [R_f = 0.35, petroleum ether–EtOAc (75:25)].

3.4. Preparation of carbamates (compounds S2–S9)[16]

To a solution of oleanolic acid (100 mg) in toluene (3 mL), an equivalent amount of benzyl isocyanate (29.0 mg) or allyl isocyanate (18.3 mg) or 4-biphenyl isocyanate (42.9 mg) or 1-naphthyl isocyanate (37.2 mg) or benzene sulfonyl isocyanate (40.7 mg), were added and the solutions were separately mixed with 15 μL of triethylamine and refluxed for 1 h. The reactions were monitored by TLC using petroleum ether–EtOAc (80:20). Water (10 mL) was then added and each reaction product was extracted with ethyl acetate (3 × 10 mL). The ethyl acetate extracts were dried over anhydrous sodium sulfate and evaporated under vacuum at 40 °C.

3.5. Purification of compounds S2–S4

Upon monitoring the reaction using TLC in case of benzyl isocyanate, it was found that it gives three products more non polar than oleanolic acid. The product was further purified by chromatography on silica gel column previously packed in petroleum ether and isocratically eluted with 10% ethyl acetate in petroleum ether. The effluents, 10 mL fractions, were monitored by TLC on silica gel plates using solvent system petroleum ether–EtOAc (80:20), and similar fractions were pooled. Sub-fractions 37–39 afforded compound **S2** [R_f = 0.62, 23 mg, 23%], Sub-fractions 45–48 afforded compound **S3** [R_f = 0.55, 25 mg, 25%], Sub-fractions 52–61 afforded compound **S4** [R_f = 0.50, 11 mg, 11%] and their purity was confirmed by TLC plate.

3.6. Purification of compound S5

TLC of the crude reaction mixture in case of allyl isocyanate revealed the presence of one product more non polar than oleanolic acid. The product was further purified by chromatography on silica

gel column previously packed in petroleum ether and isocratically eluted with 5% ethyl acetate in petroleum ether. The effluents, 10 mL fractions, were monitored by TLC on silica gel plates, and similar fractions were pooled. Sub-fractions 28–31 afforded compound **S5** [R_f = 0.71, petroleum ether–ethyl acetate (80:20), 50 mg, 50%].

3.7. Purification of compound S6

TLC of the crude reaction mixture in case of 4-biphenyl isocyanate revealed the presence of one product more non polar than oleanolic acid. The product was further purified by chromatography on silica gel column previously packed in petroleum ether and isocratically eluted with 5% ethyl acetate in petroleum ether. The effluents, 10 mL fractions, were monitored by TLC on silica gel plates, and similar fractions were pooled. Sub-fractions 21–26 afforded compound **S6** [R_f = 0.62, petroleum ether–ethyl acetate (80:20), 10 mg, 10%].

3.8. Purification of compounds S7 and S8

TLC of the crude reaction mixture in case of 1-naphthyl isocyanate revealed the presence of two products more non polar than oleanolic acid. The product was further purified by chromatography on silica gel column previously packed in petroleum ether and isocratically eluted with 5% ethyl acetate in petroleum ether. The effluents, 10 mL fractions, were monitored by TLC on silica gel plates using solvent system petroleum ether–EtOAc (80:20), and similar fractions were pooled. Sub-fractions 22–26 afforded compound **S7** [R_f = 0.67, 4 mg, 0.04%], Sub-fractions 29–40 afforded compound **S8** [R_f = 0.46, 23 mg, 23%].

3.9. Purification of compound S9

TLC of the crude reaction mixture in case of benzenesulfonyl isocyanate revealed the presence of one product more polar than oleanolic acid. The product was further purified by chromatography on silica gel column previously packed in petroleum ether and isocratically eluted with 10% ethyl acetate in petroleum ether. The effluents, 10 mL fractions, were monitored by TLC on silica gel plates, and similar fractions were pooled. Sub-fractions 73–90 afforded compound **S9** [R_f = 0.38, petroleum ether–ethyl acetate (80:20), 60 mg, 60%].

3.10. Preparation of compound S10[17]

To a solution of oleanolic acid (100 mg) in pyridine (3 mL), benzenesulfonyl chloride (40 mg) was added, and the mixture was stirred for 48 h at room temperature. The reaction was monitored by TLC using petroleum ether–ethyl acetate (80:20). The reaction was stopped by addition of water and extracted with EtOAc (3 × 10 mL). The combined EtOAc extract was dried over anhydrous sodium sulfate and evaporated under vacuum.

3.11. Purification of compound S10

TLC of the reaction mixture revealed the presence of one product. The product was further purified by chromatography on silica gel column previously packed in petroleum ether and isocratically eluted with 5% ethyl acetate in petroleum ether. The effluents, 10 mL fractions, were monitored by TLC on silica gel plates, and similar fractions were pooled. Sub-fractions 33–42 afforded compound **S10** [R_f = 0.43, petroleum ether–ethyl acetate (80:20), 12 mg, 12%].

3.12. Molecular modeling and docking

Molegro Virtual Docker (MVD, Molegro ApS, Aarhus, Denmark) is an integrated environment for studying and predicating how ligands interact with macromolecules. The identification of ligand binding modes is done by iteratively evaluating a number of candidate solutions (ligand conformations) and estimating the energy of their interaction with the macromolecule. MVD requires a three-dimensional structure of both protein and ligand.

The MolDock scoring function (MolDock Score) used by MDV is derived from the piecewise linear potential (PLP) scoring functions originally proposed by Gehlhaar et al., [18]and later extended by Yang and Chen.[19] The MolDock scoring function further improves these scoring functions with a new hydrogen bonding term and new charge schemes. The docking scoring function, E_{score}, is defined by the following energy terms;

$$E_{score} = E_{inter} + E_{intra}$$

where: E_{inter} is the ligand–protein interaction energy.

E_{intra} is the internal energy of ligand.

It is given by negative charge. The more negative the energy score (kcal/mol), more is the binding affinity.

The crystal structures of topoisomerase I and II were downloaded from RCSB Protein Data Bank (PDB 1t8i, for topoisomerase I[7]) or (PDB 1bgw, for topoisomerase II[8]). The structure in PDB format was prepared using MVD. Using MVD 6.0, the water molecules were removed and co-factor was incorporated into the protein structure was automatically prepared. The structures of the topoisomerase I and II inhibitors camptothecin (CPT) and etoposide, respectively, were used as reference molecules in docking and modeling studies. The three-dimensional structures of compounds (ligands) were first constructed using Chemsketch 12.0 software [Cambridge Soft corporation, USA], then they were energetically minimized by using Chimera 1.6.2 software with RMS gradient of 0.10 and then they were saved as mol2 format. Each of prepared ligands was submitted separately to Id Target server, and Gasteiger–Hückel charges to calculate the atomic charges of uploaded ligands.

The binding potential between topoisomerase I, II and molecules were evaluated by MVD. Scores are stated as binding free energy (E_{score} kcal/mol). The more negative the energy score (kcal/mol), more is the binding affinity.

3.13. Inhibition of DNA relaxation by topoisomerase I enzyme

Topoisomerase I drug screening kit (TopoGen, Inc., Port Orange, FL) was used to determine the inhibitory activity of **S1**–**S10** to block or reduce topoisomerase I DNA relaxation activity. For this assay, 250 ng of supercoiled plasmid DNA was added to the assay buffer (10 mM Tris–HCl, pH 7.9, 1 mM EDTA, 150 mM NaCl, 0.1% BSA, 0.1 mM spermidine, and 5% glycerol), followed by tested compound or camptothecin at a final concentration of 100 μM. Equal concentrations of DMSO were maintained in each reaction mixture so as not to produce solvent mediated inhibition of topoisomerase I activity. Topoisomerase I (2 U) was added to the assay mixture, and reactions were carried out at 37 °C for 30 min, then terminated by addition of 1% SDS (sodium dodecyl sulfate). The reaction mixtures were digested with proteinase K (50 μg/mL) for 15 min at 37 °C. DNA was separated by electrophoresis in a 1% agarose gel in TAE buffer (40 mM Tris–acetate, 1 mM EDTA) at 1 V/cm for 1–2 h at room temperature. The agarose gels were stained with ethidium bromide (0.5 μg/mL) and extensively destained in water, and the DNA bands were visualized by transillumination with UV light and quantified using imageJ software.

3.14. Inhibition of decatenation of kDNA by topoisomerase II enzyme

Compounds **S1**–**S10** were screened for the ability to inhibit the decatenation of kDNA using a Topoisomerase II assay kit (TopoGen, Inc., Port Orange, FL). Briefly, 100 μM of each compound or etoposide was incubated with kinetoplast DNA (kDNA) and 2 U topoisomerase II enzyme for 30 min at 37 °C. The reaction mixtures were digested with proteinase K (50 μg/mL) for 15 min at 37 °C. DNA was separated by electrophoresis in a 1% agarose gel in TAE buffer (40 mM Tris–acetate, 1 mM EDTA) at 1 V/cm for 1–2 h at room temperature. The agarose gels were stained with ethidium bromide (0.5 μg/mL) and extensively destained in water, and the DNA bands were visualized by transillumination with UV light and quantified using imageJ software.

3.14.1. Oleanderolide (S1)

Colorless amorphous solid, $[\alpha]_D^{24}$ +74.5 (0.2, $CHCl_3$); ^1H and ^{13}C NMR were compared with the published literature data.[11]

3.14.2. 3-*O*-[*N*-(Benzyl)carbamoyl]-oleanolic acid (S2)

Colorless amorphous solid, $[\alpha]_D^{24}$ +12.5 (0.2, $CHCl_3$); ^1H NMR (CD_3Cl_3) δ: 4.42 (br s, H-3), 5.28 (br s, H-12), 0.91 (s, H-23), 0.70 (s, H-24), 0.85 (s, H-25), 0.71 (s, H-26), 1.11 (s, H-27), 0.90 (s, H-29), 0.76 (s, H-30), 4.50 (br s, H-2′), 7.26 (m, H-4′, 8′), 7.32 (m, H-5′, 7′), 7.27 (m, H-6′); ^{13}C NMR (Table 2)

3.14.3. 3-*O*-[*N*-(Benzyl)carbamoyl]-17β-*O*-[*N*-(benzyl)carbomyl]-oleanolic acid (S3)

Colorless amorphous solid, $[\alpha]_D^{24}$ +48.6 (0.33, $CHCl_3$); ^1H NMR (CD_3Cl_3) δ: 4.42 (br s, H-3), 5.28 (br s, H-12), 0.92 (s, H-23), 0.70 (s, H-24), 0.86 (s, H-25), 0.71 (s, H-26), 1.14 (s, H-27), 0.90 (s, H-29), 0.77 (s, H-30), 4.52 (br s, H-2′), 7.34 (m, H-4′, 8′), 7.22 (m, H-5′, 7′), 7.28 (m, H-6′), 4.98 (br s, H-1″), 7.33 (m, H-3″, 7″), 7.24 (m, H-4″, 6″), 7.25 (m, H-5″); ^{13}C NMR (Table 2).

3.14.4. 17β-*O*-[*N*-(Benzyl)carbomyl]-oleanolic acid (S4)

Colorless amorphous solid, $[\alpha]_D^{24}$ +60.3 (0.33, $CHCl_3$); ^1H NMR (CD_3Cl_3) δ: 3.30 (br s, H-3), 5.30 (br s, H-12), 0.92 (s, H-23), 0.67 (s, H-24), 0.88 (s, H-25), 0.85 (s, H-26), 1.15 (s, H-27), 0.93 (s, H-29), 0.79 (s, H-30), 4.42 (br s, H-1″), 7.28 (m, H-3″, 7″), 7.32 (m, H-4″, 6″), 7.29 (m, H-5″);^{13}C NMR (Table 2).

3.14.5. 3-*O*-[*N*-(Allyl)carbamoyl]-oleanolic acid (S5)

White amorphous solid, $[\alpha]_D^{24}$ +28.5 (0.133, $CHCl_3$); ^1H NMR (CD_3Cl_3) δ: 4.38 (br s, H-3), 5.26 (br s, H-12), 0.92 (s, H-23), 0.81 (s, H-24), 0.83 (s, H-25), 1.07 (s, H-26), 1.12 (s, H-27), 0.90 (s, H-29), 0.74 (s, H-30), 3.80 (br s, H-2′), 5.38 (br s, H-3′), 5.12 (d, J = 10.2, H-4′a), 5.19 (dd, J = 16.8, 1.2, H-4′b); ^{13}C NMR (Table 2).

3.14.6. 3-*O*-[*N*-(Biphenyl)-*p*-carbamoyl]-oleanolic acid (S6)

White amorphous solid, $[\alpha]_D^{24}$ +27.5 (0.08, $CHCl_3$); ^1H NMR (CD_3Cl_3) δ: 4.52 (br s, H-3), 5.28 (br s, H-12), 0.96 (s, H-23), 0.76 (s, H-24), 0.93 (s, H-25), 0.98 (s, H-26), 1.15 (s, H-27), 0.96 (s, H-29), 0.91 (s, H-30), 7.46 (m, H-3′, 7′), 7.53 (m, H-4′, 6′), 7.57 (m, H-2″, 6″), 7.41 (m, H-3″, H-5″), 7.31 (m, H-4″); ^{13}C NMR (Table 2).

3.14.7. 3-*O*-[*N*-(1-Naphthyl)-carbamoyl]-17-β-[*N*-(1-naphthyl)-carbamoyl]-oleanolic acid (S7)

Brown amorphous solid, $[\alpha]_D^{24}$ +14.8 (0.027, $CHCl_3$); ^1H NMR (CD_3Cl_3) δ: 4.56 (br s, H-3), 5.32 (br s, H-12), 0.92 (s, H-23), 0.66 (s, H-24), 0.94 (s, H-25), 0.97 (s, H-26), 1.15 (s, H-27), 1.01 (s, H-29), 0.81 (s, H-30), 7.45 (m, H-3′, 4′), 7.62 (m, H-5′), 7.88 (m, H-6′, 9′), 7.46 (m, H-7′, 8′), 7.47 (m, H-2″, 3″), 7.85 (m, H-4″, H-8″), 8.22 (m, H-5″), 7.49 (m, H-6″, H-7″); ^{13}C NMR (Table 2).

3.14.8. 3-*O*-[*N*-(1-Naphthyl)-carbamoyl]-oleanolic acid (S8)

Brown amorphous solid, $[\alpha]_D^{24}$ +48.4 (0.33, $CHCl_3$); ^1H NMR (CD_3Cl_3) δ: 4.56 (br s, H-3), 5.28 (br s, H-12), 0.93 (s, H-23), 0.76 (s, H-24), 0.94 (s, H-25), 0.97 (s, H-26), 1.14 (s, H-27), 1.07 (s, H-29), 0.84 (s, H-30), 7.44 (m, H-3′, 4′), 7.64 (m, H-5′), 7.90 (m, H-6′),7.50 (m, H-7′, 8′), 7.85 (m, H-9′); ^{13}C NMR (Table 2).

3.14.9. 3-*O*-[*N*-(Phenylsulfonyl)-carbamoyl-17β-*N*-(phenylsulfonyl)amide]-oleanolic acid (S9)

White amorphous solid, $[\alpha]_D^{24}$ +32.5 (0.2, $CHCl_3$); ^1H NMR (CD_3Cl_3) δ: 4.56 (br s, H-3), 5.28 (br s, H-12), 0.91 (s, H-23), 0.71 (s, H-24), 0.88 (s, H-25), 0.77 (s, H-26), 1.10 (s, H-27), 0.89 (s, H-29), 0.80 (s, H-30), 7.87 (d, J = 9.0, H-3′, 7′), 7.47 (m, H-4′, 6′), 7.49 (m, H-5′),7.96 (d, J = 9.0, H-2″, 6″), 7.49 (m, H-3″, 5″), 7.51 (m, H-4″); ^{13}C NMR (Table 2).

3.14.10. 3-*O*-(Benzenesulfonyloxy)-oleanolic acid (S10)

White amorphous solid, $[\alpha]_D^{24}$ +59.3 (0.133, $CHCl_3$); ^1H NMR (CD_3Cl_3) δ: 4.28 (br s, H-3), 5.25 (br s, H-12), 0.80 (s, H-23), 0.72 (s, H-24), 0.79 (s, H-25), 0.87 (s, H-26), 1.15 (s, H-27), 0.89 (s, H-29), 0.90 (s, H-30), 7.91 (d, J = 7.2, H-2′, 6′), 7.51 (m, H-3′, 5′), 7.61 (m, H-4′);^{13}C NMR (Table 2).

4. Conclusion

Ten rationally designed analogues of oleanolic acid were synthesized on the basis of molecular modeling studies and tested for their topoisomerase I and IIα inhibitory activity. Semisynthetic reactions targeted C-3, C-28, C-12 and C-13 in oleanolic acid (Fig. 6). It was found that compounds **S2**, **S3**, **S5**, **S7** and **S9** showed greater topoisomerase I inhibitory activity than CPT. Compounds **S2**, **S3**, **S5** and **S6** showed greater activity than etoposide against topoisomerase II inhibition. Considering the previous results, we

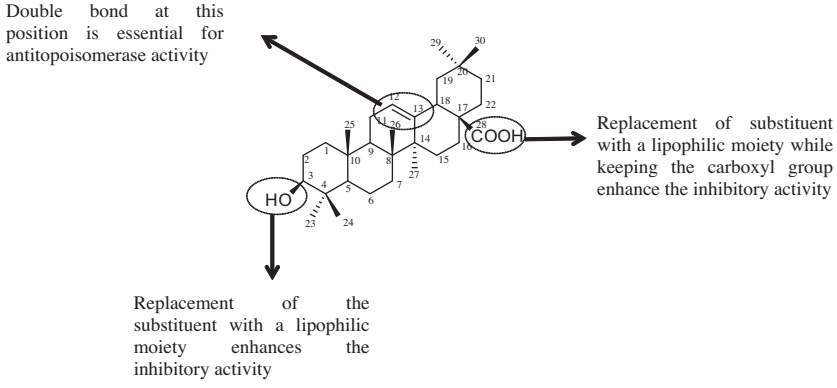

Figure 6. Summarized structure–activity relationships of oleanolic acid with regard to topoisomerase inhibition.

have concluded that we have four compounds (**S2**, **S3**, **S5** and **S7**) that have high inhibitory activities towards both topoisomerase I and II, which suggests that these compounds can act as dual inhibitors for both enzymes, thus leading to the prevention of cancer.

Acknowledgment

The Egyptian Government is acknowledged for the fellowship support to Ahmed Adel Ashour.

References

1. Pommier, Y. *ACS Chem. Biol.* **2013**, *8*, 82.
2. Syrovets, T.; Büchele, B.; Gedig, E.; Slupsky, R.; Simmet, T. *Mol. Pharmacol.* **2000**, *58*, 71.
3. Amer, M.; El-Sharkawy, S.; Marzouk, A.; Ashour, A. *J. Environ. Sci.* **2012**, *40*, 251.
4. Forterre, P.; Gribaldo, S.; Gadelle, D.; Serre, M. *Biochimie* **2007**, *89*, 427.
5. Wang, J. *Nat. Rev. Mol. Cell Biol.* **2002**, *3*, 340.
6. Deweese, J.; Osheroff, N. *Nucleic Acids Res.* **2009**, *37*, 738.
7. Staker, B.; Feese, M.; Cushman, M.; Pommier, Y.; Zembower, D.; Stewart, L.; Burgin, A. *J. Med. Chem.* **2005**, *48*, 2336.
8. Berger, J.; Gamblin, S.; Harrison, S.; Wang, J. *Nature* **1996**, *379*, 225.
9. Abdel Bar, F.; Khanfar, M.; Elnagar, A.; Liu, H.; Zaghloul, A.; Badria, F.; Sylvester, P.; Ahmed, K.; Raisch, K.; El Sayed, K. *J. Nat. Prod.* **2009**, *72*, 1643.
10. Salerno, S.; Da Settimo, F.; Taliani, S.; Simorini, F.; La Motta, C.; Fornaciari, G.; Marini, A. M. *Curr. Med. Chem.* **2010**, *17*, 4270.
11. Fu, L.; Zhang, S.; Li, N.; Wang, J.; Zhao, M.; Sakai, J.; Hasegawa, T.; Mitsui, T.; Kataoka, T.; Oka, S.; Kiuchi, M.; Hirose, K.; Ando, M. *J. Nat. Prod.* **2005**, *68*, 198.
12. Burns, D.; Reynolds, F.; Buchanan, G.; Reese, B.; Enriquez, G. *Magn. Reson. Chem.* **2000**, *38*, 488.
13. Manabe, S.; Sugioka, T.; Ito, Y. *Tetrahedron Lett.* **2007**, *48*, 787.
14. Shinkre, A.; Raisch, P.; Fan, L.; Velu, E. *Bioorg. Med. Chem. Lett.* **2007**, *17*, 2890.
15. Ballini, R.; Marcantoni, E.; Torregiani, E. *J. Nat. Prod.* **1997**, *60*, 505.
16. El Sayed, K.; Laphookhieo, S.; Yousaf, M.; Prestridge, J.; Shirode, A.; Wali, V.; Sylvester, P. *J. Nat. Prod.* **2008**, *71*, 117.
17. Merlani, M.; Amiranashvili, L.; Mulkidzhanyan, K.; Shelar, A.; Manvi, F. *Chem. Nat. Compd.* **2008**, *44*(5), 618.
18. Gehlhaar, D.; Verkhivker, G.; Rejto, P.; Fogel, D.; Fogel, L.; Freer, S. Proceedings of the Fourth International Conference on Evolutionary Programming, 1995, 615–627.
19. Yang, J.-M.; Chen, C.-C. *Proteins* **2004**, *55*, 288.